Field ionization process of Eu $4f^7 6snp$ Rydberg states*

Zhang Jing(张 婧)[a)b)], Shen Li(沈 礼)[a)b)], and Dai Chang-Jian(戴长建)[a)b)†]

[a)] *Key Laboratory of Display Materials and Photoelectric Devices, Ministry of Education, Tianjin* 300384, *China*
[b)] *School of Science, Tianjin University of Technology, Tianjin* 300384, *China*

(Received 26 March 2015; revised manuscript received 2 June 2015; published online 10 October 2015)

The field ionization process of the Eu $4f^7 6snp$ Rydberg states, converging to the first ionization limit, $4f^7 6s\ {}^9S_4$, is systematically investigated. The spectra of the Eu $4f^7 6snp$ Rydberg states are populated with three-step laser excitation, and detected by electric field ionization (EFI) method. Two different kinds of the EFI pulses are applied after laser excitation to observe the possible impacts on the EFI process. The exact EFI ionization thresholds for the $4f^7 6snp$ Rydberg states can be determined by observing the corresponding EFI spectra. In particular, some structures above the EFI threshold are found in the EFI spectra, which may be interpreted as the effect from black body radiation (BBR). Finally, the scaling law of the EFI threshold for the Eu $4f^7 6snp$ Rydberg states with the effective quantum number is built.

Keywords: Eu atom, Rydberg state, field ionization, ionization threshold

PACS: 32.30.Jc, 32.80.Ee, 32.60.+i **DOI:** 10.1088/1674-1056/24/11/113201

1. Introduction

Electric field ionization (EFI) processes in simpler atoms have been investigated extensively for the last two decades either experimentally[1–3] or theoretically.[1,4] The full-scale investigations of the EFI of Rydberg states for both alkali-metal atoms,[4–6] such as Li and Na, and alkaline-earth atoms,[7,8] e.g., Ba and Sr, have been carried out. The same is not true for rare-earth atoms, however, since the existing studies have almost all been concentrated on Yb atom, on either the EFI threshold or the dynamics of the Stark states.[9,10]

All rare-earth atoms, except for Yb, have a partially filled 4f subshell, resulting in the complicated spectra of highly excited states due to the very complex structures of the ground state.[11–13] In recent years, the spectral studies of highly excited states of the Eu atom, a typical complex rare-earth atom with electronic configuration of $[Xe]4f^7 6s^2$, in zero field have been reported,[14,15] not only on bound states,[16,17] but also on some auto-ionizing states.[18,19]

Due to the high selectivity and efficiency, the EFI method has been used for detection of highly excited states,[20,21] and determination of the first ionization limit[22] and the lifetimes of the Eu atom.[23] Obviously, the core structure of the Eu atom ultimately dominates the complexity of its properties, leading to the fact that the EFI process of the Eu atom has been hardly touched, especially the behaviors when the intensity of electric field exceeds ionization threshold. Thus, it is more challenging to extend the above studies to its EFI process, which is the goal of the present study. More explicitly, the EFI process of the Eu $4f^7 6snp$ Rydberg states is systematically investigated, including the exact EFI ionization thresholds, and the scaling law of the EFI threshold with the effective quantum number for the Eu $4f^7 6snp$ Rydberg states.

2. Experiment

In this section, both experimental setup and approach, as well as some related formulas, will be described.

The experimental setup, as shown in Fig. 1, includes three parts: a laser system, an atomic beam system, and a data acquisition system. The laser system includes three tunable dye lasers pumped by an Nd:YAG laser at wavelength of 532 nm. Each of three dye lasers has a pulse width of 5–8 ns, a line width of 0.5 cm^{-1}, and a repetition rate of 20 Hz. In order to ensure the given excitation scheme, the pulses of the second and third lasers are delayed by 8 ns and 16 ns relative to the pulse of the first laser, respectively. The polarization of three lasers is perpendicular to the direction of the electric field.

An atomic beam produced from a heated oven at 750 K ejects into the interacting region between two parallel electric field plates, 1 cm apart, on which an appropriate voltage is applied. The collimated atomic beam intersects with the laser beams to decrease the Doppler broadening effect.

The data acquisition system includes a micro-channel plate (MCP) detector, a digital pulse generator, and a pulsed HV power supply with the rise time of 100 ns and the tunable pulse width from 0.2 μs to 2.5 μs. A digital oscilloscope and a high-speed digitizer are connected with a computer. The excited atom is ionized by the pulsed electric field, 0.5 μs after the laser pulses, from which the ion is extracted by the same electric field to the MCP detector, whose signal is processed by the high-speed digitizer, and downloaded to a computer for further analysis.

*Project supported by the National Natural Science Foundation of China (Grant Nos. 11004151 and 11174218).
†Corresponding author. E-mail: daicj@126.com
© 2015 Chinese Physical Society and IOP Publishing Ltd

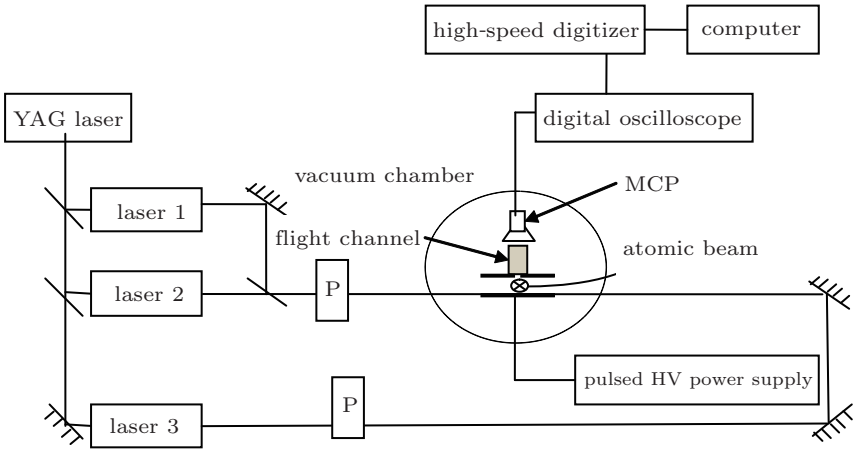


Fig. 1. (color online) Schematic diagram of the experimental setup. Here, P is a linear polarizer.

The excitation scheme, as shown in Fig. 2, is carried out with the three dye lasers. The first two lasers sequentially excite the Eu atom from the $4f^7 6s^2\ {}^8S^o_{7/2}$ ground state to the $4f^7 6s7s\ {}^8S^o_{7/2}$ state through the $4f^7 6s6p\ {}^{10}P_{9/2}$ intermediate state, where their wavelengths are fixed at 686.44 nm and 668.70 nm, respectively. The wavelength of the third laser is scanned within the range of 617–636 nm so that many Rydberg states can be populated, which can be detected by the EFI technique.

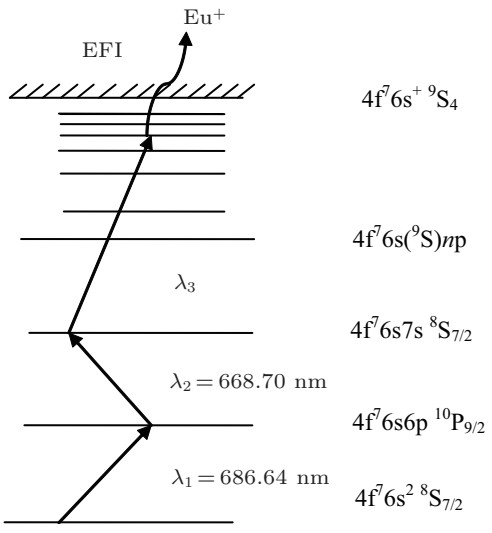


Fig. 2. The diagram of the experimental scheme.

The EFI method is well known as an effective method for detecting higher members of Rydberg states. If the strength of the electric field exceeds a critical value for a given Rydberg atom, the ionization efficiency can be up to 100%. Namely, the classical EFI threshold F for a hydrogenic atom,[10] in the atomic units, is

$$F = 1/16n^{*4}, \tag{1}$$

where n^* is the effective quantum number, which can be obtained from the Rydberg formula

$$n^* = \sqrt{\frac{R}{I_0 - E_n}}, \tag{2}$$

where $R = 109736.918\ \mathrm{cm}^{-1}$ is the mass-corrected Rydberg constant for the Eu atom; E_n is the level energy obtained from experiment; and I_0 is the ionization limit of the Eu atom.

As mentioned in the previous section, the main concern of the present study is to observe the EFI process of Eu atom. In order to carry out such an investigation, the property of the pulsed power supply has to be controlled to fulfill the EFI method. For instance, the variation of the EFI signal with the electric field strength can be obtained with the computerized power supply.

It is well known that the EFI process can be either diabatic or adiabatic, mainly depending on the rise time of the pulsed power supply used in the experiment. We have studied two different cases when atoms are field ionized: (i) field with almost constant strength, (ii) field strength is rapidly decreased.

Based on the parameters of our pulsed power supply, the rise time of 100 ns and the width varied from 0.2 μs to 2.5 μs, it enables us to observe the EFI process within the frame of the adiabatic process, while the diabatic process, requiring a slow varied and linearly rising field ramp, is not the subject of the present study.

It is worth noting that the rise time of pulsed power supply is kept at the same value of 100 ns, which enables us to study the adiabatic EFI process with two different pulse widths, 0.2 μs and 2.5 μs. The differences between the two cases mentioned above will be demonstrated and discussed in the next section.

3. Results and discussion

The experiment starts with the spectra of the Eu $4f^7 6snp$ Rydberg states, acquired by the combination of multi-step resonance excitation and the EFI technique, to obtain the exact

value of ionization threshold of Eu, as shown in Fig. 3. An overview of the $4f^7 6sn$p Rydberg series with $n = 26$ to 72 and a close-up of the highest members are shown in Figs. 3(a) and 3(b), respectively.

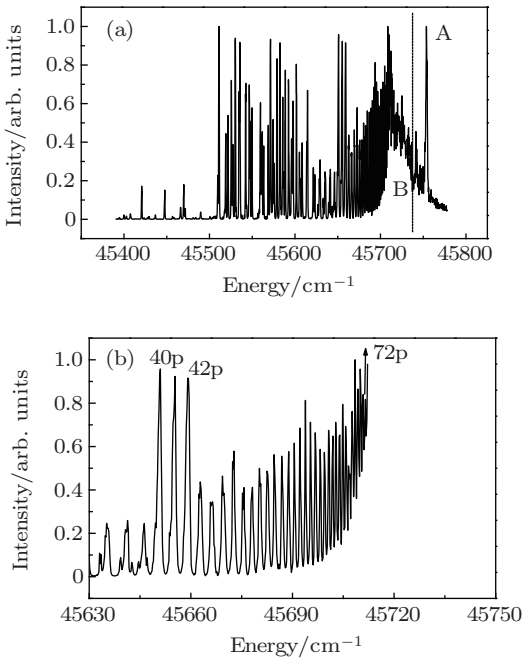


Fig. 3. The EFI spectra of the Eu $4f^7 6s(^9S)np$ Rydberg series at $F = 2$ kV·cm^{-1}. (a) An overview, and (b) the close-up. The dot line in panel (a) denotes the position of the first ionization limit.

A narrow peak, marked as A, is above the first ionization limit, while a wide profile, marked as B, is across the limit, as shown in Fig. 3(a). Obviously, both of them have a much larger width than those of bound states, which is partially due to the profound configuration interaction with the related $4f^7 6s(^9S)\varepsilon p$ continuum states, whose detailed physical mechanism was explained in the related literature.[18,19]

With the aid of the close-up of highest members shown in Fig. 3(b) and the help of the relevant literature,[20] the Eu $4f^7 6s(^9S)np\ ^8P_J$ Rydberg states with $n = 26$ to 72 are identified, based on the fact that energy corresponding to each peak is the sum of the three-step laser energy.

Turning to the observation of the EFI spectrum when the strength of electric field is continuously adjusted, we are able to examine the differences between the two cases corresponding to pulse width fixed at 0.2 μs and 2.5 μs, respectively. Taking the $4f^7 6s66p$ state at $E = 45705.74$ cm^{-1} as an example, shown in Fig. 4, the EFI signal varies with the strength of electric field. The EFI threshold F_0, corresponding to an abrupt increase in the ion current indicated by an arrow in the figure, is defined by the maximum slope of EFI signal, F_1 is defined as the EFI signal suddenly drops at a specific field strength and indicated by a dotted arrow in the figure.

Namely, for the given state, $4f^7 6s66p$, the EFI threshold is $F_0 = 32$V·cm^{-1} and 35 V·cm^{-1} in the two cases corresponding to pulse width of 2.5 μs and 0.2 μs, respectively.

Now, let us make a comparison between the two different EFI processes corresponding to the pulse width of 2.5 μs and 0.2 μs. First, the EFI threshold with pulse width of 0.2 μs is higher than that with pulse width of 2.5 μs, which is true for all Eu $4f^7 6s(^9S)np\ ^8P_J$ Rydberg states. Secondly, In the case of pulse width of 2.5 μs, the EFI signal drops suddenly at a specific field strength, $F_1 = 2815$ V·cm^{-1}, while the same phenomenon is not observed with the pulse width of 0.2 μs within 3 kV·cm^{-1}, the scale of the pulsed power supply used in experiment. This phenomenon is also true for all Eu $4f^7 6s(^9S)np\ ^8P_J$ Rydberg states. Thus, it is reasonable to assume that the same phenomenon may appear at the higher field strength, beyond 3 kV·cm^{-1}. The two different cases when atoms are field ionized: one is field with almost a constant strength, the other field strength is rapidly decreased, this leads to the differences, that are the EFI threshold with pulse width of 0.2 μs is higher than that with pulse width of 2.5 μs, and the EFI signal drops suddenly at a specific field strength only with pulse width of 2.5 μs.

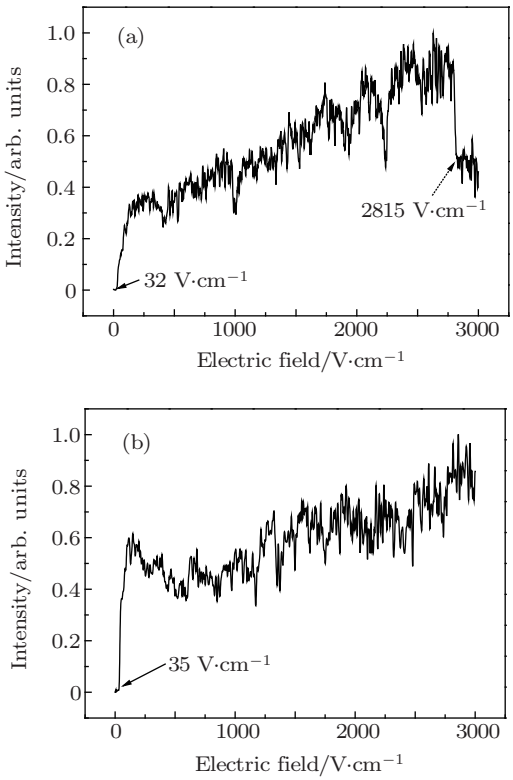


Fig. 4. The EFI process of $4f^7 6s66p\ ^8P_J$ state. The pulse width is fixed at (a) 2.5 μs and (b) 0.2 μs, respectively.

To examine the above assumption, similar observations have also been carried out for other states in the same $4f^7 6s(^9S)np$ series, such as $n = 26$ state, as shown in Fig. 5.

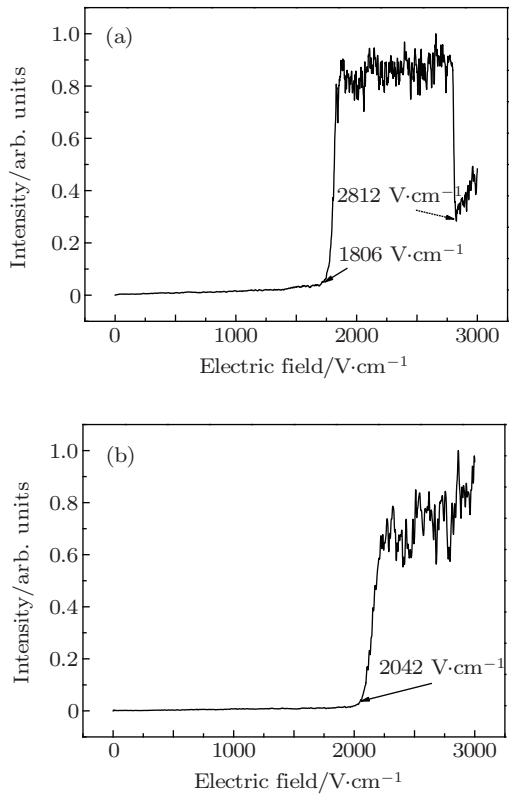


Fig. 5. The EFI process of $4f^7 6s26p\ ^8P_J$ state. The pulse width is fixed at (a) 2.5 μs and (b) 0.2 μs, respectively.

In terms of the EFI process, there is obviously a difference among the different-n states by comparing their EFI profiles. For instance, there is a flat top in the EFI profile of 26p state, while it is not the case for the 66p state. In other words, the EFI signal of 66p state reaches its maximum before dropping down, while there is no obvious maximum in the case of 26p state. To find out the reason for this, we have examined their positions in the spectrum shown in Fig. 3(a) and found that the 26p state is far away from the wide profile B, while the 66p state is superimposed on it. We have made a further step by checking all the EFI profiles of other np states, and have confirmed the above observation. This fact indicates that the wide profile B in Fig. 3(a) plays an important role on the EFI profile of the $4f^7 6s(^9S)np$ states. One may attribute this fact to their interaction with the related $4f^7 6s(^9S)\varepsilon p$ continuum states and the adjacent states.

Another observation has been made by examining the width of the EFI profiles of different np states, defined by the difference between the two thresholds, F_1–F_0, indicated by two arrows in Figs. 4(a) and 5(a). It is found that the more difference in the n values, the more in this width, which may also be seen from Table 1. In the utmost case, taking the 26p and 66p states as a pair, the EFI profile of the 66p state is much broader than that of the 26p state. In other words, the difference, F_1–F_0, is much larger for the higher states, due to the fact that F_0 is much more sensitive to the n-value than the F_1 seems to be.

Table 1. The EFI properties of the Eu $4f^7 6sn$p Rydberg states, converging to the first ionization limit, $4f^7 6s\ ^9S_4$. The pulse width is fixed at 2.5 μs.

n	E/cm^{-1}	n^*	F_0/V·cm^{-1}	F_1/V·cm^{-1}
26	45511.29	22.14	1806	2812
27	45529.97	23.14	1532	2702
27	45534.05	23.37	1527	2707
27	45535.21	23.44	1525	2710
28	45541.83	23.84	1498	2708
28	45546.17	24.11	1308	2698
28	45547.22	24.18	1305	2702
28	45549.23	24.31	1291	2707
29	45559.18	24.99	1158	2714
29	45561.35	25.15	1107	2722
29	45562.92	25.26	1091	2712
30	45570.85	25.86	967	2706
30	45574.18	26.13	939	2708
31	45582.36	26.82	936	2707
31	45585.69	27.12	837	2702
31	45586.82	27.22	827	2714
32	45592.61	27.77	808	2714
32	45596.15	28.18	707	2714
33	45601.82	28.72	696	2697
33	45605.05	29.07	617	2700
34	45614.72	30.22	532	2689
35	45621.31	31.08	470	2695
35	45622.91	31.29	452	2685
36	45629.19	32.22	400	2765
37	45635.17	33.17	361	2702
38	45640.13	34.03	321	2705
39	45645.91	35.12	283	2705
40	45651.05	36.18	251	2815
42	45659.38	38.12	207	2817
44	45666.81	40.15	185	2800
45	45670.04	41.13	158	2819
46	45672.98	42.09	140	2801
50	45683.34	46.13	99	2819
52	45686.61	47.67	84	2818
53	45688.53	48.65	82	2803
54	45690.33	49.62	74	2833
55	45691.97	50.56	69	2800
56	45693.69	51.59	64	2808
57	45695.18	52.56	57.5	2818
58	45696.75	53.64	57.3	2805
59	45697.93	54.48	48	2807
60	45697.34	55.55	44	2810
61	45700.25	56.28	41	2808
62	45701.49	57.31	38	2813
63	45702.62	58.31	36	2813
65	45704.71	60.28	34	2829
66	45705.74	61.34	32	2815
67	45706.71	62.39	28.5	2817

Now, let us discuss the possible effect from the blackbody radiation (BBR) due to the temperature of the atomic beam.[24] As shown in Fig. 6, there are some peaks superimposed on the EFI profiles.

The BBR, originated from the operating temperature at 800 K, may induce some transitions between the nearby Rydberg states. Based on the detailed analysis of the EFI spectrum of the 40p state, shown in Fig. 6, one may observe the corre-

spondence between the peaks in the EFI spectrum and the EFI thresholds of 6s*n*p Rydberg states nearby with the lower *n* values.

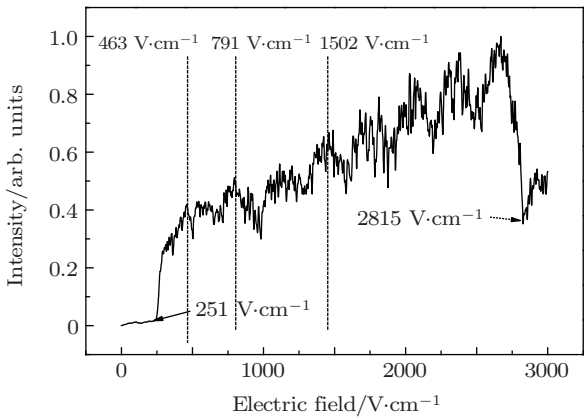


Fig. 6. The EFI process of the 4f^{7}6s40p ^{8}P$_J$ state. The pulse width is fixed at 2.5 μs.

For instance, the peaks at 463 V·cm^{-1}, 791 V·cm^{-1}, and 1502 V·cm^{-1} on the EFI profile of the 40p state are corresponding to the lower 6s*n*p states with $n = 35$, 32, and 27, respectively. The above peaks[25] are verified by the results listed in Table 1 within the error bars, which are measured individually with the EFI detection technique. The agreement between the two independent measurements mentioned above in turn interprets the mechanism of the BBR. Namely, the structures above the EFI threshold on the EFI profiles shown in Fig. 4 or Fig. 6 are indeed due to BBR effect, driving the atom from its initial state to some nearby lower states.

It is worth mentioning that the structures above the EFI threshold of 4f^{7}6s*n*p Rydberg series lead to the profile being less smooth than what it should be. There is an additional effect in the field ionization process experiment, especially for those states with the higher principal quantum number. In addition, the mutational site of the field ionization signal F_1 should be concerned with self structure of the Eu atom and is affected by the ionization efficiency.

More observations on the EFI threshold of Eu 4f^{7}6s*n*p ^{8}P$_J$ Rydberg states are systematically made,[20] as shown in Table 1. Apart from the level energies for many states with their *n* and n^* values, both the EFI threshold F_0 and the F_1, where the EFI signal drops down, are listed. As seen from the table, the variation of F_1 for different-*n* states, about 2800 V·cm^{-1}, is much smaller than those of F_0.

As shown in Table 1, it is demonstrated that for the Eu 4f^{7}6s*n*p ^{8}P$_J$ Rydberg states, the higher the state is, the easier it ionized, and the EFI threshold increases with the decrease of n^*, as expected. The F_0 and F_1 have an uncertainty of 1 V·cm^{-1}. Ionization efficiency may induce the EFI signal decline about 2800 V·cm^{-1}. Different *J* values converging to the same *n* of the Rydberg states can be distinguished in the lower energy levels of Fig. 3(a),[26] so we can see one *n* member corresponding to multiple EFI threshold F_0 in Table 1, however, the *J* value of higher *n*-value cannot be distinguished because of the line width of lasers, so higher *n*-value of the Rydberg states, one-to-one correspondence in Table 1.

In order to obtain the physical insight into the interior relations between the EFI threshold and the n^*, the effective quantum number, it is helpful to plot a diagram that shows the EFI thresholds versus n^*, for the Eu 4f^{7}6s*n*p (^{8}P$_J$) Rydberg states with $n = 26$–67, as shown in Fig. 7.

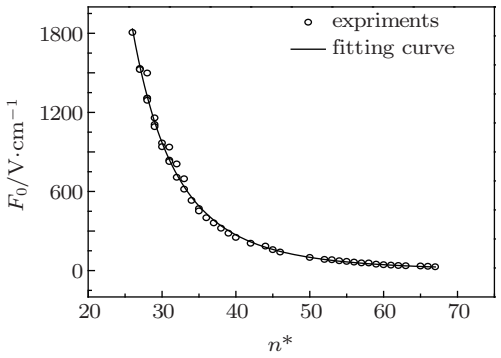


Fig. 7. The EFI thresholds versus n^* for the Eu 4f^{7}6s*n*p (^{8}P$_J$) Rydberg states.

In Fig. 7, the circles represent the experimental data of the EFI threshold, while the solid line is the curve by fitting the data to scale the n^* values. The best fit yields the scaling law for the EFI thresholds of the Eu 4f^{7}6s*n*p (^{8}P$_J$) Rydberg states, namely

$$F = 0.099(n^*)^{-4.04}. \tag{3}$$

The obvious difference from Eq. (1) indicates that the Eu atom is by no means a hydrogenic atom. Actually, it is less difficult to ionize the Eu atom than to do so for a counterpart of hydrogenic atom, reflecting the impact of quantum defects.

4. Conclusion

The electric field ionization process of the Eu 4f^{7}6s*n*p Rydberg states has been investigated with the combination of multi-step laser excitation and continuously scanning the strength of the pulsed electric field. Not only the ionization thresholds for the 42 4f^{7}6s*n*p Rydberg states are measured systematically with high precision, but also their exact turning point, where the EFI signal drops, is observed for the first time. Many characteristics of the EFI process and possible impact from the black body radiation are discussed either qualitatively or quantitatively. Apart from the observation on field ionization process of the Eu 4f^{7}6s*n*p Rydberg states, the scaling law of their ionization thresholds of the Eu atom with the n^* is also obtained for the first time.

References

[1] Zhi M C, Dai C J and Li S B 2001 *Chin. Phys.* **10** 929
[2] Liu Y P, Dai C J and Li S B 2005 *Electron. Spectrosc. Relat. Phenom* **142** 91
[3] Deng S H, Gao S, Li Y P, Xu X Y and Lin S L 2010 *Chin. Phys. B* **19** 040511
[4] Li X M, Ruan Y P and Zhong Z P 2012 *Acta Phys. Sin.* **61** 023104 (in Chinese)
[5] Menédez J M, Martín I and Velasco A M 2004 *Chem. Phys. Lett.* **398** 287
[6] Huang S Z and Chu J M 2010 *Chin. Phys. B* **19** 063101
[7] Zhong J W, Fang D W, Li J and Zhang S 2000 *J. Quant. Spectrosc. Radiat. Transfer* **67** 79
[8] Dou W D, Dai C J and Li S B 2004 *J. Quant. Spectrosc. Radiat. Transfer* **85** 145
[9] Fang D W, Dai C J, Shu X W, Li Q and Zhang S 1995 *Acta Phys. Sin.* **44** 678 (in Chinese)
[10] Dai C J, Zhang S, Shu X W, Fang D W and Li J 1995 *J. Quant. Spectrosc. Radiat. Transfer* **53** 179
[11] Shah M L, Sahoo A C, Pulhani A K, Gupta G P, Suri B M and Dev V 2014 *Eur. Phys. J. D* **68** 1
[12] Li M, Dai C J and Xie J 2011 *J. Quant. Spectrosc. Radiat. Transfer* **112** 793
[13] Xiao Y, Dai C J, Zhao H Y and Qin W J 2009 *Acta Phys. Sin.* **58** 3071 (in Chinese)
[14] Nakhate S G, Razvi M A N, Connerade J P and Ahmad S A 2000 *J. Phys. B: At. Mol. Phys.* **33** 5191
[15] Xiao Y, Dai C J and Qin W J 2010 *Chin. Phys. B* **19** 063202
[16] Smith G and Tomkins F S 1975 *Proc. R. Soc. A* **342** 149
[17] Xiao Y, Dai C J, Zhao H Y and Qin W J 2009 *Acta Phys. Sin.* **58** 3071 (in Chinese)
[18] Bhattacharyya S, Souza R D, Rao P M and Razvi M A N 2003 *Spectrochim. Acta Part B* **58** 469
[19] Bhattacharyya S, Razvi M A N, Cohen S and Nakhate S G 2007 *Phys. Rev. A* **76** 012502
[20] Xie J, Dai C J, and Li M 2011 *Chin. Opt. Lett.* **9** 050201
[21] Ye S W, Dai C J and Zhao Y H 2012 *Acta Opt. Sin.* **32** 0230001
[22] Shen L, Ye S W and Dai C J 2012 *Acta Phys. Sin.* **61** 063301 (in Chinese)
[23] Jing H, Ye S W and Dai C J 2015 *Chin. Phys. B* **24** 013203
[24] Fang D W, Xie W J and Zhang S 1997 *Acta Phys. Sin.* **46** 1888 (in Chinese)
[25] Beiting E J, Hildebrandt G F, Kellert F G, *et al.* 1979 *J. Chem. Phys.* **70** 3551
[26] Xie J, Dai C J and Li M 2011 *J. Phys. B: At. Mol. Phys.* **44** 015002